

---

# 000 SIEVE ATTENTION: FUSING CONTEXT-AWARE FILTERING 001 AND SEQUENTIAL ALLOCATION FOR LONG SEQUENCES 002

003 **Anonymous authors**

004 Paper under double-blind review

## 009 ABSTRACT

011 Transformer-based language models struggle with long-context generalization, a problem  
012 often rooted in their attention mechanisms. Existing solutions often face a trade-off: sparse  
013 attention mechanisms excel at identifying globally relevant content but are permutation-  
014 invariant and rely on brittle positional encodings, while sequential mechanisms are in-  
015 herently order-aware but can be ‘short-sighted,’ failing to attend to distant yet crucial in-  
016 formation. To resolve this dichotomy, we propose Sieve Attention, a novel, two-stage  
017 attention mechanism that unifies content-based filtering with sequential allocation. Sieve  
018 Attention first employs  $\alpha$ -entmax to ‘sieve’ the entire context, selecting a small candidate  
019 set of content-relevant tokens. Subsequently, it applies a sequential, stick-breaking pro-  
020 cess exclusively on this pre-filtered set to allocate attention with an intrinsic recency bias,  
021 thereby eliminating the need for external positional encodings. We theoretically prove that  
022 this design allows Sieve Attention to overcome the mutual limitations of its predecessors,  
023 demonstrating both immunity to local distractors and inherent order-sensitivity. Extensive  
024 experiments on long-context language modeling and retrieval benchmarks show that Sieve  
025 Attention significantly outperforms established baselines in length extrapolation and in-  
026 context learning. Our work presents a new path toward building more robust long-context  
027 models by holistically integrating global content analysis and local sequential reasoning  
028 directly within the attention mechanism. The code is available in this anonymous link.

## 029 1 INTRODUCTION

031 The Transformer has become the de facto standard for large-scale language models, demonstrating unpar-  
032 alleled capabilities across a wide range of tasks. However, as the demand for processing increasingly long  
033 documents, dialogues, and codebases grows, a fundamental limitation of the standard Transformer has be-  
034 come a critical bottleneck: its struggle with long-context generalization (Liu et al., 2023; Hu et al., 2024b;  
035 Wang et al., 2024). This challenge stems directly from the design of its core component, the softmax-based  
036 attention mechanism. We identify two primary failure modes that hinder its performance on sequences  
037 extending beyond the training length.

038 First, the softmax function inherently produces a dense probability distribution, known as sum to one and  
039 winner take all, forcing the model to allocate some attention weight to every token in the context (Maruf  
040 et al., 2019). As the sequence length increases, this leads to attention dispersion, where the attention signal is  
041 inevitably diluted across a growing number of tokens (Nakanishi, 2025). Consequently, the model’s ability  
042 to focus on a few critical pieces of information deteriorates, resulting in a sharp decline in performance  
043 on tasks that require precise information retrieval from extensive histories. As illustrated in 1 (left) on a  
044 multi-query repeated associative recall (MQRAR) task (Tan et al., 2025), the accuracy of standard softmax  
045 attention collapses as the context window expands, failing to recall. This is a common result when training  
046 long sequence models, not only in text data (Liu et al., 2024a).

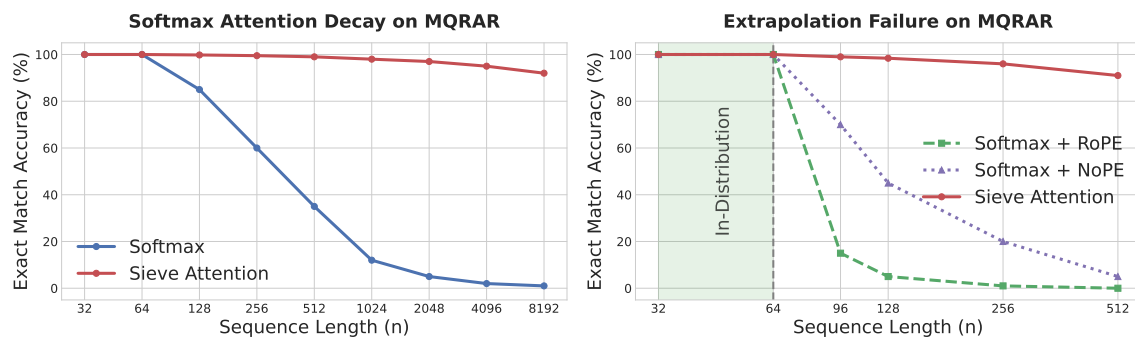


Figure 1: Failures of standard attention mechanisms on the Multi-Query Repeated Associative Recall (MQRAR) task under (left) long sequences and (right) out-of-distribution extrapolation. Sieve Attention demonstrates robust performance in both scenarios, illustrating its effectiveness.

Second, to compensate for the permutation-invariant nature of the attention mechanism, models rely on external positional encodings (PE). While methods like Rotary Positional Embeddings (RoPE) (Su et al., 2021) have been widely adopted, they exhibit poor extrapolation capabilities, failing catastrophically when presented with relative positions unseen during training (Press et al., 2021). As shown in 1 (right), the performance of a RoPE-equipped model plummets immediately beyond its training length. Removing positional encodings entirely (NoPE) offers marginal improvement but fails to provide a robust mechanism for sequential reasoning, leading to a similar decline. This reliance on brittle PEs creates a significant obstacle to true length generalization.

To address these intertwined challenges, we propose Sieve Attention, a novel attention mechanism that fundamentally redesigns how Transformers process information by unifying content-based filtering and sequential allocation. Sieve Attention operates via a two-stage process: it first employs a sparse activation function to “sieve” the entire context, filtering out irrelevant noise and selecting a small, content-relevant candidate set. Subsequently, it performs a sequential, stick-breaking allocation process exclusively on this pre-filtered set, allowing it to make a final, order-aware decision with an intrinsic recency bias. This design allows Sieve Attention to first identify what is important, regardless of distance, and then decide which of the critical items is most relevant based on sequence order, all without relying on external positional encodings.

As demonstrated in Figure 1, our method maintains high accuracy even at long sequences and exhibits powerful extrapolation capabilities. Our contributions are threefold:

- We propose Sieve Attention, a new attention mechanism that synergistically combines sparse, content-based selection with sequential, order-aware allocation, eliminating the need for PEs.
- Our theoretical analysis showing how Sieve Attention overcomes the “short-sightedness” of purely sequential mechanisms and the order-insensitivity of sparse mechanisms.
- We conduct extensive experiments on a range of long-context benchmarks, showing that Sieve Attention significantly outperforms established baselines in length extrapolation, in-context learning, and complex reasoning.

## 2 PRELIMINARY

We first establish the formal groundwork for our work. We begin by reviewing the Transformer attention mechanism, then discuss sparse attention methods designed for long-context modeling, and finally introduce a formal definition of length generalization centered on the principle of sparsity.

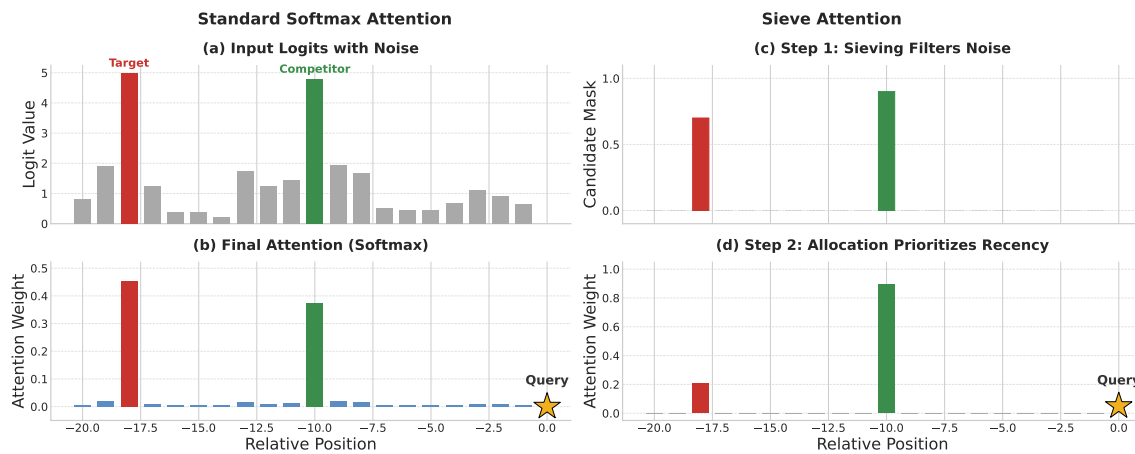


Figure 2: An illustration of the Sieve Attention mechanism compared to standard Softmax. (a) Given a context with a distant target, a closer competitor, and various noise tokens, (b) Softmax attention is diluted, assigning significant weight to both the target and competitor, as well as non-trivial weights to noise. In contrast, Sieve Attention (c) first applies a filtering step, using a sparse activation to form a candidate set containing only the target and competitor, effectively eliminating all noise. (d) Subsequently, the allocation step applies a sequential, recency-biased rule on the candidate set.

## 2.1 THE TRANSFORMER AND ATTENTION MECHANISM

The (decoder-only) Transformer architecture (Vaswani et al., 2017) processes a sequence of input tokens  $X = (x_1, \dots, x_n)$ , where each token is mapped to an embedding vector. For a given token at position  $j$ , the attention mechanism computes its output by attending to all preceding tokens  $i < j$ . This is achieved by projecting the token’s embedding into a query vector  $q_j \in \mathbb{R}^{d_k}$ , and projecting the preceding tokens’ embeddings into key vectors  $k_i \in \mathbb{R}^{d_k}$  and value vectors  $v_i \in \mathbb{R}^{d_v}$ .

The core of the mechanism is the scaled dot-product attention. The attention weights are computed by applying a normalization function  $\pi$  to the logits  $z_{i,j}$ , which measure the compatibility between the query and key vectors:

$$z_{i,j} = \frac{q_j^\top k_i}{\sqrt{d_k}} \quad \text{and} \quad a_j = \pi([z_{1,j}, \dots, z_{j-1,j}]) \quad (1)$$

The output vector  $o_j$  is then a weighted sum of the value:

$$o_j = \sum_{i=1}^{j-1} a_{i,j} v_i \quad (2)$$

In the standard Transformer, the normalization function  $\pi$  is the softmax function:

$$a_{i,j} = \text{softmax}(z_j)_i = \frac{\exp(z_{i,j})}{\sum_{k=1}^{j-1} \exp(z_{k,j})} \quad (3)$$

A key property of the softmax is that it produces a *dense* probability distribution, assigning a non-zero weight  $a_{i,j} > 0$  to every token  $i$  in the context. As we will discuss, this density is a primary source of challenges in long-context generalization, motivating the exploration of sparse alternatives.

---

141 2.2 SPARSE SOFTMAX FOR LONG SEQUENCES  
142

143 The dense nature of softmax attention becomes problematic as context length  $n$  grows. It leads to **attention**  
144 **dispersion**, where attention weights are spread thinly across a vast number of tokens, preventing the  
145 model from focusing on critical information (Nakanishi, 2025). This motivates the use of sparse attention  
146 mechanisms, which can assign exactly zero weight to irrelevant tokens, thereby creating a focused pattern.

147 A prominent family of such mechanisms is derived from  $\alpha$ -entmax Peters et al. (2019), a differentiable  
148 transformation that generalizes softmax and can produce sparse distributions. For a vector of logits  $z \in \mathbb{R}^n$   
149 and a parameter  $\alpha > 1$ ,  $\alpha$ -entmax is defined as:

150

$$151 \alpha\text{-entmax}(z)_i = [(\alpha - 1)z_i - \tau(z)]_+^{\frac{1}{\alpha-1}} \quad (4)$$

152 where  $[\cdot]_+ = \max(0, \cdot)$ , and  $\tau(z)$  is a thresholding value that ensures the resulting distribution sums to  
153 one. The key property is that any token whose scaled logit  $(\alpha - 1)z_i$  is below the threshold  $\tau(z)$  receives  
154 an attention weight of exactly zero. The degree of sparsity increases with  $\alpha$ . When  $\alpha \rightarrow 1$ ,  $\alpha$ -entmax  
155 smoothly recovers the dense softmax function, and for the special case of  $\alpha = 2$ , it becomes the well-known  
156 Sparsemax transformation Martins & Astudillo (2016). These methods provide a content-aware mechanism  
157 to enforce sparsity, allowing the model to learn to ignore irrelevant parts of the context.

158

159 3 THE SIEVE ATTENTION MECHANISM  
160

161 Building on the principle that sparsity is fundamental to length generalization, we introduce **Sieve Attention**,  
162 a novel attention mechanism designed to exploit this property explicitly. Standard attention mechanisms  
163 conflate the tasks of identifying what is important and where it is in the sequence. Sieve Attention decouples  
164 these decisions into a principled two-stage process: a content-based filtering stage followed by a sequential  
165 allocation stage. This design allows the model to first identify a sparse set of relevant tokens from the entire  
166 context, and then apply a recency-biased judgment only on this filtered set, which is illustrated in Figure 2.

167

168 3.1 STEP 1: CONTENT-AWARE FILTERING  
169

170 The first stage of Sieve Attention aims to identify the true sparse dependency set  $S^*$  as defined in our  
171 preliminary section. Given the logits  $z_j = [z_{1,j}, \dots, z_{j-1,j}]$ , instead of immediately normalizing them, we  
172 apply a sparse activation function,  $\pi_{\text{sparse}}$ , which we instantiate with  $\alpha$ -entmax (Peters et al., 2019). This  
173 function acts as a “sieve,” filtering out tokens with low relevance scores.

174 The output of this stage is a sparse, non-negative vector of candidate scores,  $c_j$ . The set of tokens with  
175 non-zero scores forms the **sparse candidate set**,  $S_j$ .

176

$$177 c_j = \alpha\text{-entmax}(z_j) \quad (5)$$

178

$$179 S_j = \{i \mid c_{i,j} > 0\} \quad (6)$$

180 Crucially, the size of this set,  $s_j = |S_j|$ , is typically much smaller than the context length ( $s_j \ll j - 1$ ). This step  
181 effectively approximates the k-sparse dependency set  $S^*$  by leveraging the global content  
182 information embedded in the logits. It ensures that only the most salient tokens, regardless of their position,  
183 are considered for the final attention.

184

185 3.2 STEP 2: SELECTIVE SEQUENTIAL ALLOCATION  
186

187 The second stage resolves any ambiguity within the candidate set  $S_j$  by applying a sequential, recency-biased  
188 allocation rule. This is achieved via a stick-breaking process, but constrained exclusively to the tokens in

188  $S_j$ . Let the elements of  $S_j$  be sorted by their position as  $i_1 < i_2 < \dots < i_{s_j}$ . The final attention weight  
 189  $a_{i_m,j}$  for a token  $i_m \in S_j$  is:

$$191 \quad a_{i_m,j} = \sigma(z_{i_m,j}) \prod_{l=m+1}^{s_j} (1 - \sigma(z_{i_l,j})) \quad (7)$$

193 where  $\sigma(\cdot)$  is the sigmoid function. For any token  $k \notin S_j$ , its attention weight is defined to be zero,  $a_{k,j} = 0$ .  
 194 This allocation process assigns attention weights based on both the token’s relevance (via  $\sigma(z_{i_m,j})$ ) and its  
 195 relative position among the other candidates. A highly relevant token that appears more recently in the  
 196 sequence will “break the stick” with a higher probability, leaving less attention mass for earlier tokens. This  
 197 mechanism introduces an inductive bias for recency without PEs.

### 198 3.3 HARDWARE-EFFICIENT IMPLEMENTATION

200 **Online  $\alpha$ -entmax:** We adapt FlashAttention’s online algorithms to compute  $\alpha$ -entmax thresholds  $\tau(z_j)$   
 201 without materializing the full logit matrix. A two-pass approach within each thread block first computes  
 202 global thresholds, then applies filtering during the second pass while computing attention outputs.

204 **In-SRAM Sequential Allocation:** After filtering identifies sparse candidates  $S_j$ , we perform in-kernel  
 205 compaction to gather candidate logits into contiguous SRAM blocks. Log-space stick-breaking is then  
 206 applied efficiently on these dense blocks:

$$207 \quad a_{i_m,j} = \exp \left( z_{i_m,j} - \sum_{k=m}^{s_j} \log(1 + \exp(z_{i_k,j})) \right)$$

210 This design ensures complexity depends on the small candidate set size  $s_j \ll L$  rather than full sequence  
 211 length, making Sieve Attention a scalable drop-in replacement for standard attention. Algorithm 1 details  
 212 the complete fused kernel implementation.

## 214 4 THEORETICAL ANALYSIS OF SIEVE ATTENTION

216 We now theoretically analyze how Sieve Attention’s two-stage design provides superior length generalization  
 217 capabilities. Our analysis is grounded in two key principles from recent literature: the importance of  
 218 *attention concentration* for avoiding representational collapse and the role of *k-sparse dependencies* in en-  
 219 abling length generalization (Golowich et al., 2025). A key lesson from prior work is that the ability of an  
 220 attention mechanism to concentrate its weights is critical for avoiding issues like representational collapse  
 221 in long contexts (Vasylchenko et al., 2025). The following proposition formalizes this.

222 **Proposition 1** (Strong Concentration Resilience). *Let  $c_j = \alpha\text{-entmax}(z_j)$  be the candidate score distribution  
 223 with support  $S_j$  and entropy  $H(c_j)$ . Let  $a_j$  be the final attention distribution. The entropy of the  
 224 final distribution is bounded by the entropy of the candidate distribution,  $H(a_j) \leq H(c_j)$ . Furthermore,  
 225 this concentration becomes stronger if a recent candidate  $i_l \in S_j$  has a sufficiently high logit such that its  
 226 activation  $\sigma(z_{i_l,j}) \rightarrow 1$ . For any earlier candidate  $i_m \in S_j$  (with  $m < l$ ), its final weight will diminish  
 227 towards zero,*

$$228 \quad a_{i_m,j} = \sigma(z_{i_m,j}) \prod_{k=m+1}^{s_j} (1 - \sigma(z_{i_k,j})) \xrightarrow{\sigma(z_{i_l,j}) \rightarrow 1} 0$$

230 because the product term contains  $(1 - \sigma(z_{i_l,j})) \rightarrow 0$ . This dynamically shrinks the support of  $a_j$  to a strict  
 231 subset of  $S_j$ , leading to stronger concentration, i.e.,  $H(a_j) < H(c_j)$ .

233 Beyond merely concentrating attention, a robust model must concentrate it on the *correct* set of tokens,  
 234 i.e., the true k-sparse dependency set  $S^*$ . This is challenging in realistic scenarios where irrelevant but

235 positionally advantageous ‘distractor’ tokens compete for attention. We now show how Sieve Attention’s  
236 global filtering stage provides a principled defense against such near-sighted distractions.  
237

238 **Proposition 2** (Robust Identification of Sparse Dependencies). *Consider a task with a  $k$ -sparse dependency  
239 structure, where the true dependency set is  $S^* \subset \{1, \dots, j-1\}$ . Let  $t_d \notin S^*$  be a distractor token and  
240  $t_f \in S^*$  be a token from the true dependency set. Even if  $t_d$  is positionally closer to the query, Sieve Attention  
241 can exclude  $t_d$  from its candidate set  $S_j$  by ensuring its logit  $z_d$  satisfies the condition:*

$$242 \quad (\alpha - 1)z_d \leq \tau(z_j)$$

243 where  $\tau(z_j)$  is the  $\alpha$ -entmax threshold. This is achieved when the true dependency token  $t_f$  has a sufficiently  
244 large logit  $z_f$ , which raises the global threshold  $\tau(z_j)$  enough to filter out  $t_d$ . In contrast, purely sequential  
245 mechanisms that lack a global filtering stage must assign a non-zero weight to  $t_d$ , thereby diminishing the  
246 weight of the more distant but correct token  $t_f$ .

247 Finally, achieving true length generalization requires not only identifying the correct sparse dependencies but  
248 also learning a decision rule for attending within that set that is itself independent of the sequence length.  
249 Standard sparse attention fails here, as it must rely on positional encodings which are known to struggle  
250 with extrapolation. We argue that Sieve Attention’s sequential allocation stage provides precisely such a  
251 length-invariant heuristic, forming the final piece of the puzzle for robust generalization.

252 **Proposition 3** (Length-Invariant Heuristics for Generalization). *The sequential allocation stage of Sieve  
253 Attention learns a length-invariant heuristic. The relative attention weight between any two candidates  
254  $t_a, t_b \in S_j$  with sorted positions  $i_a < i_b$  is governed by the relation:*

$$255 \quad \frac{a_{i_a,j}}{a_{i_b,j}} = \frac{\sigma(z_{i_a,j})}{\sigma(z_{i_b,j})} \cdot (1 - \sigma(z_{i_b,j})) \cdot \prod_{l:i_a < i_l < i_b, i_l \in S_j} (1 - \sigma(z_{i_l,j}))$$

256 This ratio depends only on the logits of tokens within the ordered candidate subset from  $i_a$  to  $i_b$ , not on the  
257 global sequence length  $j$  or their absolute positions. This promotes the learning of a compositional rule that  
258 enables  $(L, \bar{L}, \epsilon)$ -length generalization as defined in Golowich et al. (2025).

## 261 5 RELATED WORK

262 **Length Generalization in Transformers** A significant body of research has identified the limitations of  
263 standard positional encodings as a primary obstacle. While absolute positional embeddings (Vaswani et al.,  
264 2017) are inherently constrained, relative schemes like RoPE (Su et al., 2021) and ALiBi (Press et al.,  
265 2021) have shown improved, yet still limited, extrapolation capabilities. Techniques such as Positional  
266 Interpolation (Chen et al., 2023) and POSE (Zhu et al., 2024) have been proposed to mitigate these issues  
267 by modifying the encoding scheme during fine-tuning or training.

268 **Sparse Softmax Mechanisms** Other methods aim to replace the dense softmax function with transformations  
269 that can assign exactly zero weight to irrelevant tokens. A leading approach in this area is the  
270  $\alpha$ -entmax transformation (Peters et al., 2019), which provides a differentiable continuum between dense  
271 softmax ( $\alpha = 1$ ) and highly sparse activations. As demonstrated in (Vasylenko et al., 2025),  $\alpha$ -entmax can  
272 maintain a low-entropy, concentrated attention distribution even as sequence length increases.

273 **Sequential and Recency-Biased Attention** An alternative line of work has explored mechanisms with  
274 inherent sequential biases, removing the need for explicit positional encodings. One prominent approach is  
275 the State Space Model (SSM), such as S4 (Gu et al., 2021) and Mamba (Gu & Dao, 2023), which utilizes a  
276 continuous-time process with decay mechanisms. This naturally discounts information from the distant past,  
277 creating an effective recency bias (Yang et al., 2024; Liu et al., 2024b). Another such prominent mechanism  
278 is Stick-Breaking Attention (Tan et al., 2025; Shen et al., 2017), which computes attention weights via  
279 a discrete sequential process that also naturally prioritizes more recent tokens. This “recency bias” is a  
280 powerful heuristic for many language tasks where local context is paramount.

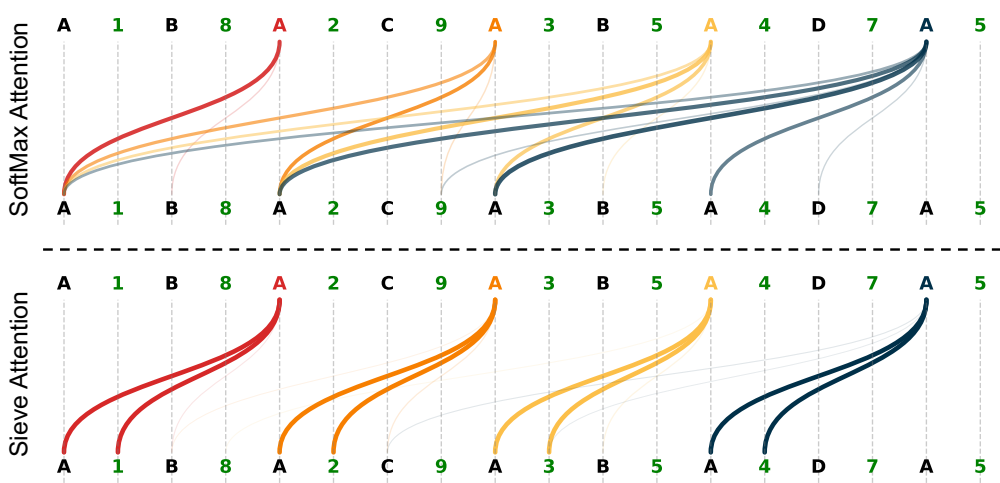


Figure 3: Attention visualization on the MQRAR task. Standard Softmax attention is distracted, assigning weights to multiple historical definitions of the variable ‘E’. Sieve Attention demonstrates clear and accurate focus, consistently attending to the most recent, correct assignment for each query.

Method	MQRAR ( $L = 4$ )						Copy ( $L = 2$ )					
	ID	4×	16×	64×	256×	1024×	ID	4×	16×	64×	256×	
Softmax+RoPE	100.0	0.5	0.0	0.0	0.0	0.0	100.0	0.0	0.0	0.0	0.0	
$\alpha$ -Entmax+RoPE	100.0	15.2	0.1	0.0	0.0	0.0	100.0	25.8	0.0	0.0	0.0	
Stick-Breaking	100.0	98.5	95.3	88.1	75.4	50.9	100.0	99.1	97.2	90.5	78.3	
<b>Sieve Attention</b>	<b>100.0</b>	<b>99.9</b>	<b>99.8</b>	<b>99.5</b>	<b>99.2</b>		<b>98.5</b>	<b>100.0</b>	<b>99.8</b>	<b>99.1</b>	<b>97.8</b>	<b>95.2</b>

Table 1: Exact match accuracy (%) on synthetic tasks. Models are trained on a sequence length of  $n = 64$ .

## 6 EXPERIMENTS

### 6.1 SYNTHETIC DATA EXPERIMENTS

Several works have utilized synthetic tasks as a probing ground for Transformers’ length-generalization capabilities (Anil et al., 2022; Dziri et al., 2023; Zhou et al., 2024). Such tasks allow precise control over training and test lengths, revealing whether a model has truly learned a scalable algorithm or merely memorized patterns. Concretely, we evaluate our models on a diverse set of synthetic tasks designed to test different aspects of long-context modeling: 1. Retrieval-focused task: We use *Multi-query Repeated Associative Recall* (MQRAR), a challenging variant of associative recall where variables are repeatedly updated (Tan et al., 2025). This task directly assesses a model’s ability to maintain focus on the most recent. 2. Memory-dependent task: We evaluate models on *Copy* on the ability of memorization.

**Experimental Setup.** All models are trained using a decoder-only Transformer architecture with a minimal number of layers to isolate the performance of the attention mechanism specifically. Our baselines include: (1) Softmax+RoPE, the standard and strong baseline; (2)  $\alpha$ -Entmax+RoPE, a sparse attention mechanism that still relies on positional encodings; and (3) Stick-Breaking, a sequential, position-encoding-free mechanism. Our proposed Sieve Attention is also position-encoding-free. For models employing RoPE, we apply a RoPE scaling factor of 16 to improve their extrapolation, providing the strongest possible baseline. All models are trained on sequences of length  $n = 64$ . Further details are described in Appendix D.

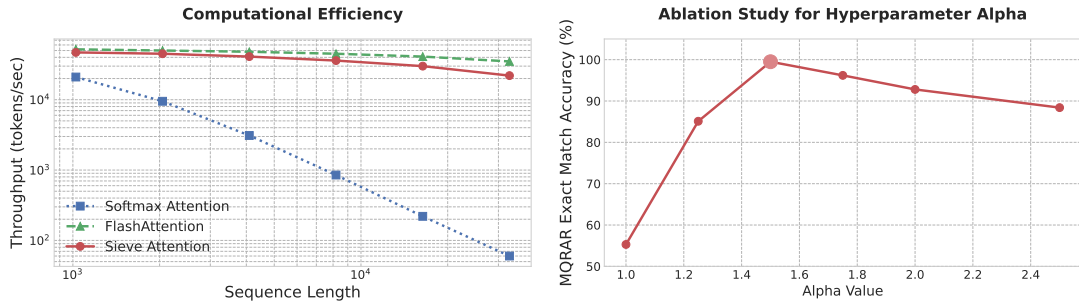


Figure 4: Ablation Studies for Sieve Attention. (Left) Computational throughput (tokens/sec) versus sequence length. (Right) Sensitivity analysis on the MQRAR task for the hyperparameter  $\alpha$  in the filtering.

Size	Model	Reasoning				Common Sense / QA			LM	
		ARC-c	ARC-e	OBQA	Avg.	Hella.	PIQA	Wino.	Avg.	Wiki.
1B	Softmax	35.8	65.6	38.8	46.7	64.8	75.0	63.4	67.7	13.8
1B	Stick-breaking	37.7	67.6	36.6	47.3	65.4	76.0	63.1	68.2	13.4
1B	<b>Sieve Attention</b>	<b>37.9</b>	<b>67.8</b>	<b>39.1</b>	<b>48.3</b>	<b>65.5</b>	<b>76.2</b>	<b>63.9</b>	<b>68.5</b>	<b>13.2</b>
3B	Softmax	42.2	73.1	40.8	52.0	73.2	78.8	67.6	73.2	11.3
3B	Stick-breaking	<b>44.9</b>	74.3	40.4	53.2	74.1	<b>79.7</b>	68.0	73.9	10.8
3B	<b>Sieve Attention</b>	44.5	<b>74.8</b>	<b>41.3</b>	<b>53.5</b>	<b>74.2</b>	79.5	<b>68.3</b>	<b>74.1</b>	<b>10.6</b>
4B	Qwen1.5	39.6	61.5	40.0	47.0	71.4	77.0	68.1	72.2	12.5

Table 2: Results on NLP benchmarks for pretrained models.

**Results on Synthetic Tasks.** The results, presented in Table 1, reveal that Sieve Attention robustly outperforms all baselines on tasks requiring precise, long-range retrieval and memory. On the MQRAR task, methods relying on RoPE fail catastrophically beyond the training length, confirming that even with sparse attention, brittle positional encodings remain a bottleneck. Stick-Breaking attention generalizes significantly better, but its performance degrades at extreme lengths, likely due to its recency bias being distracted by intermediate irrelevant tokens. In contrast, Sieve Attention achieves near-perfect accuracy up to  $1024 \times$  the training length, demonstrating that its initial filtering stage effectively removes distractors.

**Ablation Study.** First, we evaluate the computational throughput (tokens/sec) against standard Softmax Attention and the highly optimized FlashAttention Dao (2023). As shown on the left of the figure 4, Sieve Attention’s throughput is orders of magnitude higher than that of standard Softmax at longer sequence lengths. While FlashAttention remains the fastest implementation, our method is highly competitive. Second, we analyze the impact of the hyperparameter  $\alpha$  from  $\alpha$ -entmax on the MQRAR task. The right shows that model accuracy is sensitive to this choice. Performance peaks at  $\alpha = 1.5$  with nearly 100% accuracy. Performance degrades if  $\alpha$  is too low (approaching a dense softmax at  $\alpha = 1.0$ ) or too high (becoming overly sparse), indicating that  $\alpha$  provides a tunable knob for the filtering stage.

**Visualizations.** To visually inspect the behavior of our model, we trained a two-layer Transformer on MQRAR and visualized the attention patterns. As illustrated in Figure 3, the patterns produced by Sieve Attention are qualitatively superior. When retrieving the third definition of the variable ‘E’, the standard Softmax+RoPE model is distracted by the earlier, stale assignment. Its attention is split, leading to an ambiguous and incorrect retrieval. In stark contrast, Sieve Attention correctly retrieves the most recent assignment, demonstrating that its two-stage mechanism successfully filters distractors and prioritizes recency, leading to a more interpretable and accurate attention pattern.

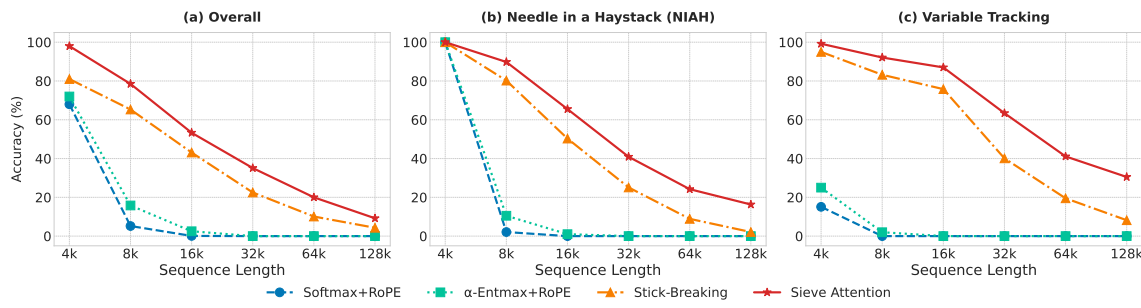


Figure 5: RULER benchmark for models with 4k context. Accuracy is evaluated on sequences up to 128k.

### 6.1.1 LANGUAGE MODEL PRETRAINING

**Setup.** We pretrain 1B and 3B parameter models using a two-stage training scheme (Hu et al., 2024a) on a 1T token corpus mixing large-scale open-source datasets. We directly compare Sieve Attention against an identically configured Softmax+RoPE baseline. We evaluate the models on a suite of standard multiple-choice QA and common sense reasoning benchmarks from the LM Evaluation Harness (Gao et al., 2023).

**Results.** As shown in Table 2, Sieve Attention models consistently outperform their Softmax+RoPE counterparts across both 1B and 3B scales. On average, Sieve Attention achieves a higher score across the board and obtains better perplexity on WikiText. This indicates that the benefits of Sieve Attention are not confined to synthetic tasks but also translate to improved performance and efficiency in large-scale pretraining.

### 6.1.2 LONG-CONTEXT EVALUATION ON RULER

**Setup.** We evaluate our pretrained 1B models on the RULER benchmark (Hsieh et al., 2024), a suite of ‘needle-in-a-haystack’ tasks designed to test the long-context retrieval capabilities of language models. Although our models were pretrained only on a 4k context window, this evaluation serves as a rigorous test of their out-of-the-box length extrapolation capabilities on 128k tokens.

**Results.** The results, shown in Figure 5, confirm the superiority of Sieve Attention in long-context scenarios. On the overall benchmark average, as well as on the specific Needle in a Haystack (NIAH) and Variable Tracking sub-tasks, Sieve Attention maintains robust performance. In contrast, methods reliant on PEs fail catastrophically. The strong performance on both NIAH and Variable Tracking further validates our core claim: Sieve Attention is effective at both filtering out irrelevant noise and maintaining precise sequential awareness (critical for Variable Tracking), making it a powerful solution for long-context modeling.

## 7 CONCLUSION

In this work, we introduced **Sieve Attention**, a novel two-stage mechanism that resolves the fundamental conflict between global, content-aware sparse attention and local, order-aware sequential attention. By decoupling the task of *what* to attend to from *how* to prioritize it, our method provides a principled path to length generalization, eliminating the need for external positional encodings.

**Limitations and Future Work.** Despite promising results, our work presents several avenues for future research. While our experiments on models up to 3B are encouraging, validating these findings on 70B+ scale models and further optimizing our computational kernel to match FlashAttention are crucial next steps. From a methodological standpoint, our model’s performance is sensitive to the sparsity-controlling hyperparameter  $\alpha$ , suggesting future work on adaptive or learned sparsity mechanisms. Furthermore, the strong recency bias from the sequential allocation stage, while effective for many tasks, may not be optimal for problems requiring more complex structures.

---

423      **ETHICS STATEMENT**

424

425      This work presents a foundational advancement in Transformer architectures for long-context processing.  
426      Our goal is to enhance the technical capabilities of language models, enabling positive applications in areas  
427      such as scientific research and information retrieval. We acknowledge that more capable language models  
428      have broader societal implications, and we advocate for their responsible development and deployment. Our  
429      research does not introduce new application-level risks; instead, it contributes to the fundamental under-  
430      standing of AI systems.

431

432      **REPRODUCIBILITY STATEMENT**

433

434      To ensure the reproducibility of our findings, we have attached the source code for Sieve Attention. The  
435      model architecture is described in the paper, and a comprehensive description of our experimental setup,  
436      including synthetic task generation, model configurations, and training hyperparameters, is provided in the  
437      Appendix. All evaluations are performed on standard, publicly available benchmarks (e.g., RULER, LM  
438      Evaluation Harness), allowing for direct and verifiable replication of our results.

439

440      **REFERENCES**

441

442      Cem Anil, Yuhuai Wu, Anders Andreassen, Aitor Lewkowycz, Vedant Misra, Vinay Ramasesh, Ambrose  
443      Sloane, Guy Gur-Ari, Ethan Dyer, and Behnam Neyshabur. Exploring length generalization in large lan-  
444      guage models, 2022. URL <https://arxiv.org/abs/2207.04901>.

445      Yonatan Bisk, Rowan Zellers, Jianfeng Gao, Yejin Choi, et al. Piqa: Reasoning about physical commonsense  
446      in natural language. In *Proceedings of the AAAI conference on artificial intelligence*, pp. 7432–7439,  
447      2020.

448      Shouyuan Chen, Sherman Wong, Liangjian Chen, and Yuandong Tian. Extending context window of  
449      large language models via positional interpolation, 2023. URL <https://arxiv.org/abs/2306.15595>.

450

451      Peter Clark, Isaac Cowhey, Oren Etzioni, Tushar Khot, Ashish Sabharwal, Carissa Schoenick, and Oyvind  
452      Tafjord. Think you have solved question answering? try arc, the ai2 reasoning challenge. *arXiv preprint*  
453      *arXiv:1803.05457*, 2018.

454

455      Tri Dao. Flashattention-2: Faster attention with better parallelism and work partitioning. *arXiv preprint*  
456      *arXiv:2307.08691*, 2023.

457

458      Nouha Dziri, Ximing Lu, Melanie Sclar, Xiang Lorraine Li, Liwei Jiang, Bill Yuchen Lin, Peter West, Chan-  
459      dra Bhagavatula, Ronan Le Bras, Jena D. Hwang, Soumya Sanyal, Sean Welleck, Xiang Ren, Allyson  
460      Ettinger, Zaid Harchaoui, and Yejin Choi. Faith and fate: Limits of transformers on compositionality,  
461      2023. URL <https://arxiv.org/abs/2305.18654>.

462

463      Leo Gao, Jonathan Tow, Baber Abbasi, Stella Biderman, Sid Black, Anthony DiPofi, Charles Foster, Lau-  
464      rence Golding, Jeffrey Hsu, Alain Le Noac'h, Haonan Li, Kyle McDonell, Niklas Muennighoff, Chris  
465      Ociepa, Jason Phang, Laria Reynolds, Hailey Schoelkopf, Aviya Skowron, Lintang Sutawika, Eric Tang,  
466      Anish Thite, Ben Wang, Kevin Wang, and Andy Zou. A framework for few-shot language model evalua-  
467      tion, 12 2023. URL <https://zenodo.org/records/10256836>.

468

469      Noah Golowich, Samy Jelassi, David Brandfonbrener, Sham M. Kakade, and Eran Malach. The role of  
470      sparsity for length generalization in transformers, 2025. URL <https://arxiv.org/abs/2502.16792>.

---

470 Aaron Grattafiori, Abhimanyu Dubey, Abhinav Jauhri, Abhinav Pandey, Abhishek Kadian, Ahmad Al-  
471 Dahle, Aiesha Letman, Akhil Mathur, Alan Schelten, Alex Vaughan, Amy Yang, Angela Fan, Anirudh  
472 Goyal, Anthony Hartshorn, Aobo Yang, Archi Mitra, Archie Sravankumar, Artem Korenev, Arthur  
473 Hinsvark, Arun Rao, Aston Zhang, Aurelien Rodriguez, Austen Gregerson, Ava Spataru, Baptiste  
474 Roziere, Bethany Biron, Binh Tang, Bobbie Chern, Charlotte Caucheteux, Chaya Nayak, Chloe Bi,  
475 Chris Marra, Chris McConnell, Christian Keller, Christophe Touret, Chunyang Wu, Corinne Wong, Cris-  
476 tian Canton Ferrer, Cyrus Nikolaidis, Damien Allonsius, Daniel Song, Danielle Pintz, Danny Livshits,  
477 Danny Wyatt, David Esiobu, Dhruv Choudhary, Dhruv Mahajan, Diego Garcia-Olano, Diego Perino,  
478 Dieuwke Hupkes, Egor Lakomkin, Ehab AlBadawy, Elina Lobanova, Emily Dinan, Eric Michael Smith,  
479 Filip Radenovic, Francisco Guzmán, Frank Zhang, Gabriel Synnaeve, Gabrielle Lee, Georgia Lewis An-  
480 derson, Govind Thattai, Graeme Nail, Gregoire Mialon, Guan Pang, Guillem Cucurell, Hailey Nguyen,  
481 Hannah Korevaar, Hu Xu, Hugo Touvron, Iliyan Zarov, Imanol Arrieta Ibarra, Isabel Kloumann, Ishan  
482 Misra, Ivan Evtimov, Jack Zhang, Jade Copet, Jaewon Lee, Jan Geffert, Jana Vranes, Jason Park, Jay Ma-  
483 hadeokar, Jeet Shah, Jelmer van der Linde, Jennifer Billock, Jenny Hong, Jenya Lee, Jeremy Fu, Jianfeng  
484 Chi, Jianyu Huang, Jiawen Liu, Jie Wang, Jiecao Yu, Joanna Bitton, Joe Spisak, Jongsoo Park, Joseph  
485 Rocca, Joshua Johnstun, Joshua Saxe, Junteng Jia, Kalyan Vasuden Alwala, Karthik Prasad, Kartikeya  
486 Upasani, Kate Plawiak, Ke Li, Kenneth Heafield, Kevin Stone, Khalid El-Arini, Krithika Iyer, Kshitiz  
487 Malik, Kuenley Chiu, Kunal Bhalla, Kushal Lakhota, Lauren Rantala-Yeary, Laurens van der Maaten,  
488 Lawrence Chen, Liang Tan, Liz Jenkins, Louis Martin, Lovish Madaan, Lubo Malo, Lukas Blecher,  
489 Lukas Landzaat, Luke de Oliveira, Madeline Muzzi, Mahesh Pasupuleti, Mannat Singh, Manohar Paluri,  
490 Marcin Kardas, Maria Tsimpoukelli, Mathew Oldham, Mathieu Rita, Maya Pavlova, Melanie Kambadur,  
491 Mike Lewis, Min Si, Mitesh Kumar Singh, Mona Hassan, Naman Goyal, Narjes Torabi, Nikolay Bash-  
492 lykov, Nikolay Bogoychev, Niladri Chatterji, Ning Zhang, Olivier Duchenne, Onur Çelebi, Patrick Al-  
493 rassy, Pengchuan Zhang, Pengwei Li, Petar Vasic, Peter Weng, Prajwal Bhargava, Pratik Dubal, Praveen  
494 Krishnan, Punit Singh Koura, Puxin Xu, Qing He, Qingxiao Dong, Ragavan Srinivasan, Raj Ganapathy,  
495 Ramon Calderer, Ricardo Silveira Cabral, Robert Stojnic, Roberta Raileanu, Rohan Maheswari, Rohit  
496 Girdhar, Rohit Patel, Romain Sauvestre, Ronnie Polidoro, Roshan Sumbaly, Ross Taylor, Ruan Silva, Rui  
497 Hou, Rui Wang, Saghar Hosseini, Sahana Chennabasappa, Sanjay Singh, Sean Bell, Seohyun Sonia Kim,  
498 Sergey Edunov, Shaoliang Nie, Sharan Narang, Sharath Raparth, Sheng Shen, Shengye Wan, Shruti  
499 Bhosale, Shun Zhang, Simon Vandenhende, Soumya Batra, Spencer Whitman, Sten Sootla, Stephane  
500 Collot, Suchin Gururangan, Sydney Borodinsky, Tamar Herman, Tara Fowler, Tarek Sheasha, Thomas  
501 Georgiou, Thomas Scialom, Tobias Speckbacher, Todor Mihaylov, Tong Xiao, Ujjwal Karn, Vedanuj  
502 Goswami, Vibhor Gupta, Vignesh Ramanathan, Viktor Kerkez, Vincent Gonguet, Virginie Do, Vish Voge-  
503 ti, Vitor Albiero, Vladan Petrovic, Weiwei Chu, Wenhan Xiong, Wenyin Fu, Whitney Meers, Xavier  
504 Martinet, Xiaodong Wang, Xiaofang Wang, Xiaoqing Ellen Tan, Xide Xia, Xinfeng Xie, Xuchao Jia,  
505 Xuewei Wang, Yaelle Goldschlag, Yashesh Gaur, Yasmine Babaei, Yi Wen, Yiwen Song, Yuchen Zhang,  
506 Yue Li, Yuning Mao, Zacharie Delpierre Coudert, Zheng Yan, Zhengxing Chen, Zoe Papakipos, Aad-  
507 diya Singh, Aayushi Srivastava, Abha Jain, Adam Kelsey, Adam Shajnfeld, Adithya Gangidi, Adolfo  
508 Victoria, Ahuva Goldstand, Ajay Menon, Ajay Sharma, Alex Boesenberg, Alexei Baevski, Allie Fein-  
509 stein, Amanda Kallet, Amit Sangani, Amos Teo, Anam Yunus, Andrei Lupu, Andres Alvarado, Andrew  
510 Caples, Andrew Gu, Andrew Ho, Andrew Poulton, Andrew Ryan, Ankit Ramchandani, Annie Dong, An-  
511 nie Franco, Anuj Goyal, Aparajita Saraf, Arkabandhu Chowdhury, Ashley Gabriel, Ashwin Bharambe,  
512 Assaf Eisenman, Azadeh Yazdan, Beau James, Ben Maurer, Benjamin Leonhardi, Bernie Huang, Beth  
513 Loyd, Beto De Paola, Bhargavi Paranjape, Bing Liu, Bo Wu, Boyu Ni, Braden Hancock, Bram Wasti,  
514 Brandon Spence, Brani Stojkovic, Brian Gamido, Britt Montalvo, Carl Parker, Carly Burton, Catalina  
515 Mejia, Ce Liu, Changhan Wang, Changkyu Kim, Chao Zhou, Chester Hu, Ching-Hsiang Chu, Chris Cai,  
516 Chris Tindal, Christoph Feichtenhofer, Cynthia Gao, Damon Civin, Dana Beaty, Daniel Kreymer, Daniel  
Li, David Adkins, David Xu, Davide Testuggine, Delia David, Devi Parikh, Diana Liskovich, Didem Foss,  
Dingkang Wang, Duc Le, Dustin Holland, Edward Dowling, Eissa Jamil, Elaine Montgomery, Eleonora  
Presani, Emily Hahn, Emily Wood, Eric-Tuan Le, Erik Brinkman, Esteban Arcaute, Evan Dunbar, Evan

---

517 Smothers, Fei Sun, Felix Kreuk, Feng Tian, Filippos Kokkinos, Firat Ozgenel, Francesco Caggioni, Frank  
518 Kanayet, Frank Seide, Gabriela Medina Florez, Gabriella Schwarz, Gada Badeer, Georgia Swee, Gil  
519 Halpern, Grant Herman, Grigory Sizov, Guangyi, Zhang, Guna Lakshminarayanan, Hakan Inan, Hamid  
520 Shojanazeri, Han Zou, Hannah Wang, Hanwen Zha, Haroun Habeeb, Harrison Rudolph, Helen Suk,  
521 Henry Aspegen, Hunter Goldman, Hongyuan Zhan, Ibrahim Damlaj, Igor Molybog, Igor Tufanov, Il-  
522 iias Leontiadis, Irina-Elena Veliche, Itai Gat, Jake Weissman, James Geboski, James Kohli, Janice Lam,  
523 Japhet Asher, Jean-Baptiste Gaya, Jeff Marcus, Jeff Tang, Jennifer Chan, Jenny Zhen, Jeremy Reizenstein,  
524 Jeremy Teboul, Jessica Zhong, Jian Jin, Jingyi Yang, Joe Cummings, Jon Carvill, Jon Shepard, Jonathan  
525 McPhie, Jonathan Torres, Josh Ginsburg, Junjie Wang, Kai Wu, Kam Hou U, Karan Saxena, Kartikay  
526 Khandelwal, Katayoun Zand, Kathy Matosich, Kaushik Veeraraghavan, Kelly Michelena, Keqian Li, Ki-  
527 ran Jagadeesh, Kun Huang, Kunal Chawla, Kyle Huang, Lailin Chen, Lakshya Garg, Lavender A, Leandro  
528 Silva, Lee Bell, Lei Zhang, Liangpeng Guo, Licheng Yu, Liron Moshkovich, Luca Wehrstedt, Madian  
529 Khabsa, Manav Avalani, Manish Bhatt, Martynas Mankus, Matan Hasson, Matthew Lennie, Matthias  
530 Reso, Maxim Groshev, Maxim Naumov, Maya Lathi, Meghan Keneally, Miao Liu, Michael L. Seltzer,  
531 Michal Valko, Michelle Restrepo, Mihi Patel, Mik Vyatskov, Mikayel Samvelyan, Mike Clark, Mike  
532 Macey, Mike Wang, Miquel Jubert Hermoso, Mo Metanat, Mohammad Rastegari, Munish Bansal, Nand-  
533 hini Santhanam, Natascha Parks, Natasha White, Navyata Bawa, Nayan Singhal, Nick Egebo, Nicolas  
534 Usunier, Nikhil Mehta, Nikolay Pavlovich Laptev, Ning Dong, Norman Cheng, Oleg Chernoguz, Olivia  
535 Hart, Omkar Salpekar, Ozlem Kalinli, Parkin Kent, Parth Parekh, Paul Saab, Pavan Balaji, Pedro Rittner,  
536 Philip Bontrager, Pierre Roux, Piotr Dollar, Polina Zvyagina, Prashant Ratanchandani, Pritish Yuvraj,  
537 Qian Liang, Rachad Alao, Rachel Rodriguez, Rafi Ayub, Raghotham Murthy, Raghu Nayani, Rahul Mi-  
538 tra, Rangaprabhu Parthasarathy, Raymond Li, Rebekkah Hogan, Robin Battey, Rocky Wang, Russ Howes,  
539 Ruty Rinott, Sachin Mehta, Sachin Siby, Sai Jayesh Bondu, Samyak Datta, Sara Chugh, Sara Hunt, Sargun  
540 Dhillon, Sasha Sidorov, Satadru Pan, Saurabh Mahajan, Saurabh Verma, Seiji Yamamoto, Sharadh  
541 Ramaswamy, Shaun Lindsay, Shaun Lindsay, Sheng Feng, Shenghao Lin, Shengxin Cindy Zha, Shishir Patil,  
542 Shiva Shankar, Shuqiang Zhang, Shuqiang Zhang, Sinong Wang, Sneha Agarwal, Soji Sajuyigbe, Soumith  
543 Chintala, Stephanie Max, Stephen Chen, Steve Kehoe, Steve Satterfield, Sudarshan Govindaprasad, Sumit  
544 Gupta, Summer Deng, Sungmin Cho, Sunny Virk, Suraj Subramanian, Sy Choudhury, Sydney Goldman,  
545 Tal Remez, Tamar Glaser, Tamara Best, Thilo Koehler, Thomas Robinson, Tianhe Li, Tianjun Zhang, Tim  
546 Matthews, Timothy Chou, Tzook Shaked, Varun Vontimitta, Victoria Ajayi, Victoria Montanez, Vijai Mo-  
547 han, Vinay Satish Kumar, Vishal Mangla, Vlad Ionescu, Vlad Poenaru, Vlad Tiberiu Mihaiescu, Vladimir  
548 Ivanov, Wei Li, Wencheng Wang, Wenwen Jiang, Wes Bouaziz, Will Constable, Xiaocheng Tang, Xiaojian  
549 Wu, Xiaolan Wang, Xilun Wu, Xinbo Gao, Yaniv Kleinman, Yanjun Chen, Ye Hu, Ye Jia, Ye Qi, Yenda  
550 Li, Yilin Zhang, Ying Zhang, Yossi Adi, Youngjin Nam, Yu, Wang, Yu Zhao, Yuchen Hao, Yundi Qian,  
Yunlu Li, Yuzi He, Zach Rait, Zachary DeVito, Zef Rosnbrick, Zhaoduo Wen, Zhenyu Yang, Zhiwei Zhao,  
and Zhiyu Ma. The llama 3 herd of models, 2024. URL <https://arxiv.org/abs/2407.21783>.

551 Albert Gu and Tri Dao. Mamba: Linear-time sequence modeling with selective state spaces. *arXiv preprint*  
552 *arXiv:2312.00752*, 2023.

554 Albert Gu, Karan Goel, and Christopher Ré. Efficiently modeling long sequences with structured state  
555 spaces. *arXiv preprint arXiv:2111.00396*, 2021.

557 Cheng-Ping Hsieh, Simeng Sun, Samuel Kriman, Shantanu Acharya, Dima Rekesh, Fei Jia, and Boris  
558 Ginsburg. Ruler: What's the real context size of your long-context language models? *arXiv preprint*  
559 *arXiv:2404.06654*, 2024.

561 Shengding Hu, Yuge Tu, Xu Han, Chaoqun He, Ganqu Cui, Xiang Long, Zhi Zheng, Yewei Fang, Yuxiang  
562 Huang, Weilin Zhao, et al. Minicpm: Unveiling the potential of small language models with scalable  
563 training strategies. *arXiv preprint arXiv:2404.06395*, 2024a.

---

564 Zhiyuan Hu, Yuliang Liu, Jinman Zhao, Suyuchen Wang, Yan Wang, Wei Shen, Qing Gu, Anh Tuan Luu,  
565 See-Kiong Ng, Zhiwei Jiang, and Bryan Hooi. Longrecipe: Recipe for efficient long context generaliza-  
566 tion in large language models, 2024b. URL <https://arxiv.org/abs/2409.00509>.

567 Amirhossein Kazemnejad, Inkit Padhi, Karthikeyan Natesan Ramamurthy, Payel Das, and Siva Reddy. The  
568 impact of positional encoding on length generalization in transformers. *Advances in Neural Information  
569 Processing Systems*, 36:24892–24928, 2023.

570 Guokun Lai, Qizhe Xie, Hanxiao Liu, Yiming Yang, and Eduard Hovy. Race: Large-scale reading compre-  
571 hension dataset from examinations. *arXiv preprint arXiv:1704.04683*, 2017.

572 Nelson F. Liu, Kevin Lin, John Hewitt, Ashwin Paranjape, Michele Bevilacqua, Fabio Petroni, and Percy  
573 Liang. Lost in the middle: How language models use long contexts, 2023. URL <https://arxiv.org/abs/2307.03172>.

574 Zicheng Liu, Jiahui Li, Siyuan Li, Zelin Zang, Cheng Tan, Yufei Huang, Yajing Bai, and Stan Z. Li. Gen-  
575 bench: A benchmarking suite for systematic evaluation of genomic foundation models, 2024a. URL  
576 <https://arxiv.org/abs/2406.01627>.

577 Zicheng Liu, Siyuan Li, Li Wang, Zedong Wang, Yunfan Liu, and Stan Z Li. Short-long convolutions help  
578 hardware-efficient linear attention to focus on long sequences. *arXiv preprint arXiv:2406.08128*, 2024b.

579 André F. T. Martins and Ramón Fernandez Astudillo. From softmax to sparsemax: A sparse model of  
580 attention and multi-label classification, 2016. URL <https://arxiv.org/abs/1602.02068>.

581 Sameen Maruf, André FT Martins, and Gholamreza Haffari. Selective attention for context-aware neural  
582 machine translation. *arXiv preprint arXiv:1903.08788*, 2019.

583 Stephen Merity, Caiming Xiong, James Bradbury, and Richard Socher. Pointer sentinel mixture models,  
584 2016. URL <https://arxiv.org/abs/1609.07843>.

585 Todor Mihaylov, Peter Clark, Tushar Khot, and Ashish Sabharwal. Can a suit of armor conduct electricity?  
586 a new dataset for open book question answering. *arXiv preprint arXiv:1809.02789*, 2018.

587 Ken M. Nakanishi. Scalable-softmax is superior for attention, 2025. URL <https://arxiv.org/abs/2501.19399>.

588 Ben Peters, Vlad Niculae, and André F. T. Martins. Sparse sequence-to-sequence models, 2019. URL  
589 <https://arxiv.org/abs/1905.05702>.

590 Ofir Press, Noah Smith, and Mike Lewis. Train short, test long: Attention with linear biases enables input  
591 length extrapolation. In *International Conference on Learning Representations*, 2021.

592 Keisuke Sakaguchi, Ronan Le Bras, Chandra Bhagavatula, and Yejin Choi. Winogrande: An adversarial  
593 winograd schema challenge at scale. *Communications of the ACM*, 64(9):99–106, 2021.

594 Yikang Shen, Zhouhan Lin, Chin-Wei Huang, and Aaron Courville. Neural language modeling by jointly  
595 learning syntax and lexicon. *arXiv preprint arXiv:1711.02013*, 2017.

596 Jianlin Su, Yu Lu, Shengfeng Pan, Ahmed Murtadha, Bo Wen, and Yunfeng Liu. Roformer: Enhanced  
597 transformer with rotary position embedding. *arXiv preprint arXiv:2104.09864*, 2021.

598 Shawn Tan, Songlin Yang, Aaron Courville, Rameswar Panda, and Yikang Shen. Scaling stick-breaking  
599 attention: An efficient implementation and in-depth study, 2025. URL <https://arxiv.org/abs/2410.17980>.

---

611 Ashish Vaswani, Noam Shazeer, Niki Parmar, Jakob Uszkoreit, Llion Jones, Aidan N Gomez, Łukasz Kaiser,  
612 and Illia Polosukhin. Attention is all you need. *Advances in neural information processing systems*, 30,  
613 2017.

614 Pavlo Vasylenko, Marcos Treviso, and André F. T. Martins. Long-context generalization with sparse attention,  
615 2025. URL <https://arxiv.org/abs/2506.16640>.

616 Jie Wang, Tao Ji, Yuanbin Wu, Hang Yan, Tao Gui, Qi Zhang, Xuanjing Huang, and Xiaoling Wang. Length  
617 generalization of causal transformers without position encoding. *arXiv preprint arXiv:2404.12224*, 2024.

618 Songlin Yang, Jan Kautz, and Ali Hatamizadeh. Gated delta networks: Improving mamba2 with delta rule.  
619 *arXiv preprint arXiv:2412.06464*, 2024.

620 Rowan Zellers, Ari Holtzman, Yonatan Bisk, Ali Farhadi, and Yejin Choi. Hellaswag: Can a machine really  
621 finish your sentence? *arXiv preprint arXiv:1905.07830*, 2019.

622 Hattie Zhou, Arwen Bradley, Eta Littwin, Noam Razin, Omid Saremi, Joshua M. Susskind, Samy Bengio,  
623 and Preetum Nakkiran. What algorithms can transformers learn? a study in length generalization. In *The  
624 Twelfth International Conference on Learning Representations*, 2024. URL <https://openreview.net/forum?id=AssIuHnmHX>.

625 Dawei Zhu, Nan Yang, Liang Wang, Yifan Song, Wenhao Wu, Furu Wei, and Sujian Li. Pose: Efficient  
626 context window extension of llms via positional skip-wise training, 2024. URL <https://arxiv.org/abs/2309.10400>.

627  
628  
629  
630  
631  
632  
633  
634  
635  
636  
637  
638  
639  
640  
641  
642  
643  
644  
645  
646  
647  
648  
649  
650  
651  
652  
653  
654  
655  
656  
657

---

658 **A APPENDIX OF SIEVE ATTENTION**
659

660 **B PROOFS**
661

662 *Proof of Proposition 1.* Let  $\mathcal{S}_j = \{i_1 < i_2 < \dots < i_{s_j}\}$  be the sorted candidate set. Consider the case  
663 where for some  $l \in \{1, \dots, s_j\}$ , the activation of a recent candidate approaches one, i.e.,  $\sigma(z_{i_l,j}) \rightarrow 1$ .

664 For any earlier candidate  $i_m \in \mathcal{S}_j$  where  $m < l$ , its attention weight is:

665 
$$a_{i_m,j} = \sigma(z_{i_m,j}) \cdot (1 - \sigma(z_{i_{m+1},j})) \cdots (1 - \sigma(z_{i_l,j})) \cdots (1 - \sigma(z_{i_{s_j},j}))$$
666

667 Since the product contains the term  $(1 - \sigma(z_{i_l,j}))$ , and  $(1 - \sigma(z_{i_l,j})) \rightarrow 0$ , it follows that:

668 
$$\forall m < l, \quad a_{i_m,j} \rightarrow 0$$
669

670 This implies the support of the final attention distribution  $a_j$  shrinks to a strict subset of  $\mathcal{S}_j$ :

671 
$$\text{supp}(a_j) \subseteq \{i_k \in \mathcal{S}_j \mid k \geq l\} \implies |\text{supp}(a_j)| < |\mathcal{S}_j|$$
672

673 Given that entropy  $H(p) \leq \log |\text{supp}(p)|$ , we have  $H(a_j) \leq \log |\text{supp}(a_j)| < \log |\mathcal{S}_j|$ . This demonstrates a  
674 stronger concentration, leading to  $H(a_j) < H(c_j)$ .  $\square$ 
675

676 *Proof of Proposition 2.* A token  $i$  is included in the candidate set  $\mathcal{S}_j$  if and only if  $(\alpha - 1)z_i > \tau(z_j)$ ,  
677 where  $\tau(z_j)$  is the  $\alpha$ -entmax threshold (Peters et al., 2019). A distractor token  $t_d$  is therefore excluded if  
678  $(\alpha - 1)z_d \leq \tau(z_j)$ .

679 The threshold  $\tau(z_j)$  is a monotonically increasing function of the logit vector  $z_j$ . Let  $z_j$  be a logit vector  
680 and consider another vector  $z'_j$  where only the logit of a true dependency token  $t_f \in S^*$  is increased, i.e.,  
681  $z'_f > z_f$  and  $z'_k = z_k$  for  $k \neq f$ . This implies  $\tau(z'_j) \geq \tau(z_j)$ .

682 Therefore, a sufficiently large logit  $z_f$  can raise the threshold  $\tau(z_j)$  to satisfy the exclusion condition for  $t_d$ ,  
683 even if  $z_d$  is non-trivial. This ensures  $d \notin \mathcal{S}_j$ . In contrast, a purely sequential mechanism lacking this global  
684 filtering stage would necessarily assign non-zero weight to  $t_d$ , suppressing the weight of the more distant  
685 target  $t_f$ .  $\square$ 
686

687 *Proof of Proposition 3.* For any two candidates  $t_a, t_b \in \mathcal{S}_j$  at sorted positions  $i_a < i_b$ , their attention weights  
688 are defined as:

689 
$$a_{i_a,j} = \sigma(z_{i_a,j}) \prod_{k=a+1}^{s_j} (1 - \sigma(z_{i_k,j}))$$
690
$$a_{i_b,j} = \sigma(z_{i_b,j}) \prod_{k=b+1}^{s_j} (1 - \sigma(z_{i_k,j}))$$
691

692 By splitting the product term for  $a_{i_a,j}$ , we can express it in terms of the product for  $a_{i_b,j}$ :

693 
$$\prod_{k=a+1}^{s_j} (1 - \sigma(z_{i_k,j})) = \left( \prod_{k=a+1}^b (1 - \sigma(z_{i_k,j})) \right) \cdot \left( \prod_{k=b+1}^{s_j} (1 - \sigma(z_{i_k,j})) \right)$$
694

695 Taking the ratio of the two weights cancels the common term  $\prod_{k=b+1}^{s_j} (\dots)$ , yielding:

696 
$$\frac{a_{i_a,j}}{a_{i_b,j}} = \frac{\sigma(z_{i_a,j}) \cdot \prod_{k=a+1}^b (1 - \sigma(z_{i_k,j}))}{\sigma(z_{i_b,j})}$$
697

705 which simplifies to the expression in the proposition:

$$707 \quad \frac{a_{i_a,j}}{a_{i_b,j}} = \frac{\sigma(z_{i_a,j})}{\sigma(z_{i_b,j})} \cdot (1 - \sigma(z_{i_b,j})) \cdot \prod_{l:i_a < i_l < i_b, i_l \in \mathcal{S}_j} (1 - \sigma(z_{i_l,j}))$$

709 The ratio depends only on the logits of tokens within  $\mathcal{S}_j$  between positions  $i_a$  and  $i_b$ . It is independent  
710 of the global sequence length  $j$  or the absolute positions of the candidates, thus proving the heuristic is  
711 length-invariant.  $\square$

## 713 C HARDWARE-EFFICIENT IMPLEMENTATION OF SIEVE ATTENTION

---

### 715 Algorithm 1 Fused Sieve Attention Kernel

---

717 **Input:** Query  $Q$ , Key  $K$ , Value  $V \in \mathbb{R}^{B \times H \times L \times D}$   
 718 **Input:** Block sizes  $M_B, N_B$  (adaptive based on  $L$ )  
 719 **Output:** Output  $O \in \mathbb{R}^{B \times H \times L \times D}$

720 1: **Kernel Launch:** Grid =  $(B, H, \lceil L/M_B \rceil)$ , each thread block processes  $M_B$  queries  
 721 2: **Thread Block** ( $b, h, m$ ): Load  $q_m \leftarrow Q[b, h, m M_B : (m+1) M_B, :]$   
 722 3: Initialize filtering thresholds:  $\tau \leftarrow (-\infty, \dots, -\infty) \in \mathbb{R}^{M_B}$   
 723 4: **for**  $n = 0$  **to**  $L - N_B$  **step**  $N_B$  **do** ▷ Iterate over key blocks  
 724 5: Load  $k_n \leftarrow K[b, h, n : n + N_B, :]$  with boundary mask  
 725 6: Compute  $z \leftarrow q_m k_n^T / \sqrt{D}$ , apply causal mask  
 726 7: Update  $\tau \leftarrow \max(\tau, \text{rowmax}(z))$  ▷ Online threshold computation  
 727 8: **end for**  
 728 9: Initialize:  $o \leftarrow \mathbf{0}_{M_B \times D}$ ,  $\gamma \leftarrow \mathbf{0}_{M_B}$  ▷ Output accumulator, log remaining mass  
 729 10: **for**  $n = 0$  **to**  $L - N_B$  **step**  $N_B$  **do**  
 730 11: Load  $k_n, v_n \leftarrow K[n : n + N_B], V[n : n + N_B]$  with boundary masks  
 731 12: Recompute  $z \leftarrow q_m k_n^T / \sqrt{D}$ , apply causal mask  
 732 13: *Content filtering:*  $\mathcal{S} \leftarrow \{(i, j) : z_{ij} \geq \tau_i - \epsilon\}$   
 733 14: *Sequential allocation:*  $\log p \leftarrow z + \gamma + \text{cumsum}(-\text{softplus}(z))$   
 734 15: *Apply masks:*  $\log p \leftarrow \text{mask}(\log p, \text{causal} \wedge \mathcal{S})$   
 735 16:  $o \leftarrow o + \exp(\log p) \cdot v_n$  ▷ Fused attention computation  
 736 17:  $\gamma \leftarrow \gamma + \text{rowsum}(-\text{softplus}(z))$  ▷ Update remaining mass  
 737 18: **end for**  
 738 19: **Store:**  $O[b, h, m M_B : (m+1) M_B, :] \leftarrow o$   
 739 20: Recompute forward pass information ( $\tau$ , attention probabilities)  
 740 21: Initialize:  $\frac{\partial L}{\partial q} \leftarrow \mathbf{0}$ , load  $\frac{\partial L}{\partial o}$   
 741 22: **for**  $n = 0$  **to**  $L - N_B$  **step**  $N_B$  **do**  
 742 23: Compute  $\frac{\partial L}{\partial p} \leftarrow \frac{\partial L}{\partial o} v_n^T, \frac{\partial L}{\partial z}$  via chain rule  
 743 24:  $\frac{\partial L}{\partial q} += \frac{\partial L}{\partial z} k_n^T$  ▷ Query gradients  
 744 25: **AtomicAdd:**  $\frac{\partial L}{\partial V}[n : n + N_B] += p^T \frac{\partial L}{\partial o}$  ▷ Value gradients  
 745 26: **AtomicAdd:**  $\frac{\partial L}{\partial K}[n : n + N_B] += \frac{\partial L}{\partial z} q_m$  ▷ Key gradients  
 746 27: **end for**

---

747 **Key Hardware Optimizations**

748 1. **Kernel Fusion:** All operations (filtering, allocation, output computation) execute in a single GPU  
 749 kernel, eliminating intermediate memory transfers.

---

752 2. **Online  $\alpha$ -Entmax:** Filtering thresholds computed on-the-fly without materializing the  $O(L^2)$  at-  
 753 tention matrix.

754 3. **Block Tiling:** Memory access pattern designed for  $(M_B, N_B, D)$  blocks fitting in GPU shared  
 755 memory, achieving  $O(L)$  complexity.

756 4. **Log-Space Numerics:** Stick-breaking allocation performed in log-space using softplus for numer-  
 757 ical stability.

758 5. **Atomic Gradient Updates:** Thread-safe accumulation of gradients for shared key/value parame-  
 759 ters using hardware atomic operations.

760 6. **Adaptive Block Sizing:** Block dimensions automatically adjusted based on sequence length to  
 761 satisfy hardware constraints ( $M_B, N_B \geq 16$  for Triton).

762

763 **Complexity Analysis**

764 **Time:**  $O(L^2 D / (M_B N_B))$  for attention computation plus  $O(sLD)$  for candidate processing, where  $s \ll$   
 765  $L$  is the average sparsity.

766 **Memory:**  $O(LD + M_B N_B D)$  - linear scaling with sequence length, constant overhead for block buffers.

767 **Memory Savings:** Up to 99.9% reduction vs. standard  $O(L^2)$  attention for long sequences ( $L \geq 16k$ ).

773 **D EXPERIMENTAL DETAILS**

774 **D.1 SYNTHETIC TASK DETAILS**

775 **Multi-Query Repeated Associative Recall (MQRAR).** MQRAR is a generative task designed to test a  
 776 model’s ability to track the state of variables that are updated multiple times within a long context. An input  
 777 sequence consists of a series of key-value pair assignments (e.g., ‘E 3’, ‘B 6’, ‘E 2’), followed by a series of  
 778 queries for specific keys (e.g., ‘E’, ‘B’, ‘E’). The model’s task is to output the *most recent* value assigned to  
 779 each queried key. This setup directly probes the model’s capacity to filter out stale information and focus on  
 780 the latest relevant assignment, a critical capability for tasks like code completion or dialogue modeling.

781 **Copy.** This is a standard generative task for testing a model’s memory and length generalization Kazem-  
 782 nejad et al. (2023). The model is given a sequence of tokens and must reproduce it exactly. We use a small  
 783 vocabulary size of 32 to increase the likelihood of repeated tokens, which poses a greater challenge to the  
 784 model’s positional reasoning as sequence length increases.

785 **D.2 SYNTHETIC MODEL AND TRAINING SETUP**

786 **Models.** All synthetic tasks are trained with a decoder-only Transformer. We use a minimal number of  
 787 layers (2 to 4, depending on the task) to isolate the performance of the attention mechanism itself, rather  
 788 than the scaling capabilities of deeper models. For experiments with RoPE, we use the Hugging Face  
 789 implementation from Llama 3 Grattafiori et al. (2024). To improve length extrapolation in RoPE-based  
 790 models, we apply a scaling factor of 16. For our experiments with  $\alpha$ -entmax, we use  $\alpha = 1.5$ . We use 16  
 791 attention heads for both MQRAR and Copy tasks.

792 **Training.** For optimization, we use the AdamW optimizer with default betas and a cosine learning-rate  
 793 scheduler with 10K warm-up steps. We do not employ dropout or weight decay. All models are trained

799 using bfloat16 precision. Given that even models achieving 100% in-distribution accuracy can benefit from  
800 further training, the best checkpoint is selected based on performance at  $8\times$  the in-distribution sequence  
801 length. We evaluate using exact match accuracy on 1,000 samples for each sequence length. All models are  
802 trained from scratch with 3 different random seeds, and we report the results from the best-performing run.  
803

804  
805 Table 3: Synthetic task details and hyperparameters.

Task	Samples	Batch	Vocab.	Layers	Hid. dim.
MQRAR	20M	128	256	2	256
Copy	20M	128	32	2	256

810  
811 **D.3 REAL-WORLD PRETRAINING DETAILS**  
812

813 **Model Configurations.** Our pretrained models are based on a standard decoder-only Transformer archi-  
814 tecture. The specific hyperparameters for the 1B and 3B parameter models are detailed in Table 4. All  
815 models were trained using the same vocabulary and tokenizer for fair comparison.  
816

817 Table 4: Model configurations for our 1B and 3B parameter models.  
818

Hyperparameter	1B Model	3B Model
Hidden Dimension ( $d_{\text{model}}$ )	2048	3072
Number of Layers ( $L$ )	24	32
Number of Attention Heads	32	32
FFN Intermediate Size	8192	8192
Vocabulary Size	32,000	32,000
Activation Function	GeLU	GeLU

827 **Evaluation Benchmark Details.** All real-world data evaluations were conducted using the LM Evaluation  
828 Harness framework (Gao et al., 2023). Below are brief descriptions of the benchmarks used in our pretraining  
829 evaluation (Table 2).  
830

- 831 • ARC (AI2 Reasoning Challenge) (Clark et al., 2018): A collection of grade-school level, multiple-  
832 choice science questions. We report on both the Challenge (ARC-c) and Easy (ARC-e) sets.
- 833 • Hellaswag (Zellers et al., 2019): A commonsense reasoning benchmark that involves choosing the  
834 most plausible continuation of a given sentence.
- 835 • OBQA (OpenBookQA) (Mihaylov et al., 2018): An open-book question answering dataset that  
836 requires reasoning over a small set of common knowledge facts.
- 837 • PIQA (Physical Interaction QA) (Bisk et al., 2020): A commonsense reasoning benchmark focused  
838 on understanding physical interactions and choosing the more plausible of two given solutions.
- 839 • RACE (Lai et al., 2017): A large-scale reading comprehension dataset collected from English ex-  
840 aminations for middle and high school students in China.
- 841 • Winogrande (Sakaguchi et al., 2021): An adversarial version of the Winograd Schema Challenge,  
842 designed to be robust against dataset biases for commonsense reasoning.
- 843 • Wikitext PPL (Perplexity): We measure the perplexity on the Wikitext-103 dataset (Merity et al.,  
844 2016), a standard benchmark for evaluating the language modeling capabilities of a model.  
845

---

## 846 USE OF LLM

847

848 We only apply LLM for checking spelling and grammar.

849

850

851

852

853

854

855

856

857

858

859

860

861

862

863

864

865

866

867

868

869

870

871

872

873

874

875

876

877

878

879

880

881

882

883

884

885

886

887

888

889

890

891

892